Well-Defined Carboxyl-Terminated Alkyl Monolayers Grafted onto H—Si(111): Packing Density from a Combined AFM and Quantitative IR Study

ARTICLE *in* LANGMUIR · FEBRUARY 2006

Impact Factor: 4.46 · DOI: 10.1021/la052145v · Source: PubMed

7 AUTHORS, INCLUDING:

Anne Chantal Gouget
French National Centre for Scientific Research
34 PUBLICATIONS **753** CITATIONS
SEE PROFILE

Catherine Henry de Villeneuve
French National Centre for Scientific Research
37 PUBLICATIONS **1,433** CITATIONS
SEE PROFILE

Rabah Boukherroub
French National Centre for Scientific Research
449 PUBLICATIONS **7,407** CITATIONS
SEE PROFILE

Well-Defined Carboxyl-Terminated Alkyl Monolayers Grafted onto H−Si(111): Packing Density from a Combined AFM and Quantitative IR Study

Anne Faucheux,[†,‡] Anne Chantal Gouget-Laemmel,*[,†] Catherine Henry de Villeneuve,[†] Rabah Boukherroub,[§] François Ozanam,[†] Philippe Allongue,[†] and Jean-Noël Chazalviel[†]

Laboratoire de Physique de la Matière Condensée, CNRS-Ecole Polytechnique, Route de Saclay, 91128 Palaiseau Cedex, France, STMicroelectronics, 850 rue Jean Monnet, 38926 Crolles Cedex, France, and Institut de Recherche Interdisciplinaire, IEMN, Avenue Poincaré, BP69, 59652 Villeneuve d'Ascq Cedex, France

Received August 5, 2005. In Final Form: October 28, 2005

This work demonstrates that well-defined mixed carboxyl-terminated/methyl-terminated alkyl monolayers can be prepared in one step on H-terminated Si(111) via direct photochemical hydrosilylation of undecylenic acid and 1-decene mixtures. As evidenced by AFM imaging and IR spectroscopy, a final rinse in hot acetic acid leaves the functionalized surface atomically smooth and perfectly free of physisorbed contaminants while unwanted material remains atop the monolayer with most other common solvents. The compositional surface chemistry was determined from a truly *quantitative* IR (ATR geometry) study in the range of 900−4000 cm^{-1}. Results prove that neither surface oxidation nor grafting through the carboxyl end groups occurs. Monolayers are fairly dense for such bulky end groups, with a *total* molecular surface density of ∼2.7 10^{14} cm^{-2} corresponding to a surface coverage of 0.35 (maximum theoretical value ∼0.5). Careful analysis of the CH- and COOH-related IR bands reveals that the composition of the grafted layers is richer in acid chains than the starting grafting mixture. A simple model is presented that shows that the grafting kinetics is about twice as fast for undecylenic acid as for 1-decene. Complementary electrochemical impedance measurements indicate the excellent electronic properties of the interface with a very low density of gap states. They also show that the acid terminal groups promote the penetration of water in the outer part of the organic film.

1. Introduction

Densely packed organic layers directly bonded to crystalline silicon surfaces (without an interfacial silicon oxide layer) have received increasing interest because of their variety of applications in microelectronics as well as for chemical and biochemical sensors.[1−3] Among the various chemical and electrochemical methods investigated, the hydrosilylation route via thermal, catalytic, or photochemical activation[4−10] allows the rapid formation of monolayers through Si−C covalent bonds by the reaction of ω-functionalized 1-alkene precursors with hydrogen-passivated silicon (Scheme 1).

Scheme 1

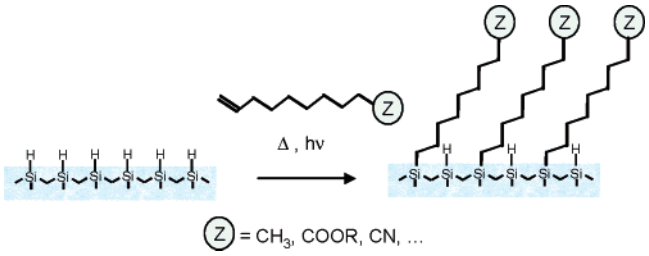

The choice of functional end group Z is restricted by its chemical reactivity toward the silicon surface. For example, −OH-, −CHO-, or $-NH_2$-terminated alkyl monolayers cannot be obtained directly by the reaction in Scheme 1 because the formation of Si−O−C or Si−N−C linkages is competing with the addition to the C═C double bond.[11−16] In these cases, the surface must first be reacted with a precursor bearing the protected end group, and deprotection is subsequently performed on the surface-immobilized species.[17−20] For the same reasons, acid-

* Corresponding author. E-mail: anne-chantal.gouget@polytechnique.fr.
† CNRS-Ecole Polytechnique.
‡ STMicroelectronics.
§ Institut de Recherche Interdisciplinaire.

(1) Buriak, J. M. *Chem. Rev.* **2002**, *102*, 1271−1308.
(2) Wayner, D. D. M.; Wolkow, R. A. *J. Chem. Soc., Perkin Trans. 2* **2002**, *2*, 23−34.
(3) Schöning, M. J.; Lüth, H. *Phys. Status Solidi A* **2001**, *185*, 65−77.
(4) Linford, M. R.; Fenter, P.; Eisenberger, P. M.; Chidsey, C. E. D. *J. Am. Chem. Soc.* **1995**, *117*, 3145−3155.
(5) Buriak, J. M.; Stewart, M. P.; Geders, T. W.; Allen, M. J.; Choi, H. C.; Smith, J.; Raftery, D.; Canham, L. T. *J. Am. Chem. Soc.* **1999**, *121*, 11491−11502.
(6) Sieval, A. B.; Demirel, A. L.; Nissink, J. W. M.; Linford, M. R.; van der Maas, J. H.; de Jeu, W. H.; Zuilhof, H.; Sudhölter, E. J. R. *Langmuir* **1998**, *14*, 1759−1768.
(7) Boukherroub, R.; Morin, S.; Bensebaa, F.; Wayner, D. D. M. *Langmuir* **1999**, *15*, 3831−3835.
(8) Bateman, J. E.; Eagling, R. D.; Worrall, D. R.; Horrocks, B. R.; Houlton, A. *Angew. Chem., Int. Ed.* **1998**, *37*, 2683−2685.
(9) Cicero, R. L.; Linford, M. R.; Chidsey, C. E. D. *Langmuir* **2000**, *16*, 5688−5695.
(10) Jin, H.; Kinser, C. R.; Bertin, P. A.; Kramer, D. E.; Libera, J. A.; Hersam, M. C.; Nguyen, S. T.; Bedzyk, M. J. *Langmuir* **2004**, *20*, 6252−6258.
(11) Bateman, J. E.; Eagling, R. D.; Horrocks, B. R.; Houlton, A. *J. Phys. Chem. B* **2000**, *104*, 5557−5565.
(12) Effenberger, F.; Götz, G.; Bidlingmaier, B.; Wezstein, M. *Angew. Chem., Int. Ed.* **1998**, *37*, 2462−2464.
(13) Boukherroub, R.; Morin S.; Sharpe, P.; Wayner, D. D. M.; Allongue, P. *Langmuir* **2000**, *16*, 7429−7434.
(14) Hacker, C. A.; Anderson, K. A.; Richter, L. J., Richter, C. A. *Langmuir* **2005**, *21*, 882−889.
(15) Zhu, X. Y.; Mulder, J. A.; Bergerson, W. F. *Langmuir* **1999**, *15*, 8147−8154.
(16) Lin, Z.; Strother, T.; Cai, W.; Cao, X.; Smith, L. M.; Hamers, R. J. *Langmuir* **2002**, *18*, 788−796.
(17) Sieval, A. B.; Linke, R.; Heij, G.; Meijer, G.; Zuilhof, H.; Sudhölter, E. J. R. *Langmuir* **2001**, *17*, 7554−7559.
(18) Coffinier, Y.; Olivier, C.; Perzyna, A.; Grandidier, B.; Wallart, X.; Durand, J.-O.; Melnyk, O.; Stiévenard, D. *Langmuir* **2005**, *21*, 1489−1496.
(19) Pike, A. R.; Lie, L. H.; Eagling, R. A.; Ryder, L. C.; Patole, S. N.; Connolly, B. A.; Horrocks, B. R.; Houlton, A. *Angew. Chem., Int. Ed.* **2002**, *41*, 615−617.

10.1021/la052145v CCC: $33.50
Published on Web 12/07/2005

terminated alkyl monolayers have long been prepared by the hydrolysis of ester-terminated alkyl monolayers because it was thought that the carboxyl end groups were also reacting with the silicon surface (formation of siloxane esters SiO(CO)R).[6] This strategy was used in particular for the binding of complex organic or biological molecules.[21−25] The disadvantage of this technique is the difficulty in achieving complete hydrolysis of the ester terminal group, the final surfaces containing both ester and acid end groups.[26] However, the direct formation of acid-terminated alkyl layers was demonstrated with porous silicon using thermal- and microwave-activated hydrosilylation with undecylenic acid.[27,28] It was also reported that the photochemical hydrosilylation of undecylenic acid on a hydrogen-terminated crystalline silicon surface does not lead to appreciable reaction between the carboxyl groups and the surface.[29] Finally, a recent paper concluded that the direct photochemical (UV) hydrosilylation of ω-alkenoic acids on H−Si(111) is possible for short irradiation times but that a reaction with the carboxyl may occur at longer times.[30]

The above brief review shows the difficulty of assessing the actual state of acid-terminated alkyl monolayers obtained in one step by hydrosilylation of ω-alkenoic acids on a H-terminated silicon surface. It is the purpose of the present article to demonstrate unambiguously and quantitatively that dense, well-defined layers can indeed be formed. Our approach makes use of a combination of AFM observations, IR spectroscopy, and impedance measurements. The photochemical reaction was performed on atomically flat H-terminated Si(111) surfaces to allow for a true quantitative analysis in terms of surface density and for easy detection of the presence of any unwanted physisorbed species by AFM imaging. IR spectroscopy was performed over an extended wavenumber range (900−4000 cm^{-1}) to examine both the possible reaction of the COOH end groups with the hydrogenated silicon surface and the degree of surface oxidation after reaction. Careful calibration of the IR intensity was performed to determine quantitatively the surface density of the grafted molecular film as a function of the volume concentration of undecylenic acid in 1-decene. The electrical behavior of the modified interface was also investigated using electrochemical impedance measurements.

2. Experimental Section

General Information. Undecylenic acid (98%), 1-decene (94%), pentane (99+%, HPLC), and ammonium sulfite monohydrate (92%) were purchased from Aldrich. 1-Decene was passed through a magnesium silicate (Florisil) column (pentane eluant) and stored under argon. All cleaning (H_2O_2, 30%; H_2SO_4, 96%; acetic acid, 100%) and etching (NH_4F, 40%) reagents were of VLSI grade and supplied by Merck.

The silicon samples were cut either from n-type (5−10 Ω cm) one-side polished silicon (111) wafers (Siltronix, France) with a miscut 0.2° toward the (11$\bar{2}$) direction or from double-side polished float zone 800 Ω cm n-type (111) silicon (Siltronix, France).

Photochemical Hydrosilylation Reaction. The Si(111) sample was cleaned in a 1/3 H_2O_2/H_2SO_4 piranha solution at 100 °C for 30 min and then rinsed copiously with ultrapure (Milli-Q) water. The atomically smooth H-terminated surface[31,32] was obtained by chemical etching for 10 min in oxygen-free 40% NH_4F (ca. 0.05 mol L^{-1} ammonium sulfite was added to the etching solution). During this time, neat undecylenic acid or 1-decene or a mixture of undecylenic acid/1-decene was outgassed under argon in a Schlenk tube at 90 °C for 30 min and then cooled to room temperature. After rinsing with ultrapure water, the H−Si(111) substrate was transferred into the Schlenk tube with continuous argon bubbling for 30 min and irradiated for 3 h in a UV reactor (6 mW cm^{-2}, 312 nm). The functionalized surface was finally rinsed with different solvents and blown dry under argon.

Infrared Spectroscopy. ATR-FTIR spectra were recorded using a Bomem MB100 FTIR spectrometer equipped with a liquid-nitrogen-cooled MCT photovoltaic detector. Spectra were recorded with s and p polarization over the 900−4000 cm^{-1} spectral range (4 cm^{-1} resolution). This extended spectral range is required to allow good signal sensitivity in the region of interest for siloxane esters and silicon oxide. It was made possible by using small samples (17.5 mm width, 520 μm thickness), which allows us to reduce the optical path length in silicon (hence a lower bulk-Si absorption below 1500 cm^{-1}) while keeping a reasonable number of internal reflections. A typical sample with 45° bevels on the two opposite sides gives 34 reflections. These prisms were prepared from double-side polished float zone 800 Ω cm n-type (111) silicon (Siltronix). In all of the figures, the reference spectrum is always a freshly prepared H−Si(111) surface. The spectra with s and p polarization were *quantitatively* analyzed as exposed in the Appendix to derive the molecular surface density.

Capacitance−Potential *C*(*V*) Measurements. The electrochemical measurements were performed in a homemade three-electrode Teflon cell connected to a potentiostat (PGSTAT10, Eco Chemie BV, The Netherlands) coupled to a frequency response analyzer. The counter electrode was a Pt wire, and the reference electrode was a Pd wire loaded with hydrogen. (The Pd wire was polarized for 10 min in 0.1 M H_2SO_4 at −2 V against the counter electrode.) The working electrode was pressed against an opening in the cell bottom using an O-ring seal (viton). The electrolyte was a 0.1 M solution of H_2SO_4. Nitrogen was bubbled through the solution to remove dissolved O_2. The impedance of the interface was measured in the accumulation regime using a 25 mV sine wave potential modulation in the frequency range of 0.2−20 kHz. The capacitance of the interface was determined from the out-of-phase part of the impedance.

Contact Mode AFM Imaging. AFM images were obtained using a Pico SPM microscope (Molecular Imaging, Phoenix, AZ) in contact mode with silicon nitride cantilevers (Nanoprobe, spring constant = 0.2 Nm^{-1}) and in a N_2 atmosphere.

3. Results and Discussion

In what follows, a V% acid-terminated monolayer or sample will designate a Si(111) surface that has been grafted in an undecylenic acid/1-decene mixture (neat products) in which the volume fraction of undecylenic acid is V%.

3.1. Preparation of Well-Defined Acid-Terminated Monolayers. Figure 1 shows the AFM image and infrared spectrum of a decyl monolayer prepared by UV irradiation of neat 1-decene

(20) Strother, T.; Cai, W.; Zhao, X.; Hamers, R. J.; Smith, L. M. *J. Am. Chem. Soc.* **2000**, *122*, 1205−1209.
(21) Boukherroub, R.; Wayner, D. D. M. *J. Am. Chem. Soc.* **1999**, *121*, 11513−11515.
(22) Wojtyk, J. T. C.; Morin, K. A.; Boukherroub, R.; Wayner, D. D. M. *Langmuir* **2002**, *18*, 6081−6087.
(23) Yu, W. H.; Kang, E. T.; Neoh, K. G.; Zhu, S. *J. Phys. Chem. B* **2003**, *107*, 10198−10205.
(24) Wagner, P.; Nock, S.; Spudich, J. A.; Volkmuth, W. D.; Chu, S.; Cicero, R. L.; Wade, C. P.; Linford, M. R.; Chidsey, C. E. D. *J. Struct. Biol.* **1997**, *119*, 189−201.
(25) Wei, F.; Sun, B.; Guo, Y.; Zhao, X. S. *Biosens. Bioelectron.* **2003**, *18*, 1157−1163.
(26) Liu, Y.-J.; Navasero, N. M.; Yu, H.-Z. *Langmuir* **2004**, *20*, 4039−4050.
(27) Boukherroub, R.; Wojtyk, J. T. C.; Wayner, D. D. M.; Lockwood, D. J. *J. Electrochem. Soc.* **2002**, *149*, H59−H63.
(28) Boukherroub, R.; Petit, A.; Loupy, A.; Chazalviel, J.-N.; Ozanam, F. *J. Phys. Chem. B* **2003**, *107*, 13459−13462.
(29) Voicu, R.; Boukherroub, R.; Bartzoka, V.; Ward, T.; Wojtyk, J. T. C.; Wayner, D. D. M. *Langmuir* **2004**, *20*, 11713−11720.
(30) Asanuma, H.; Lopinsky, G. P.; Yu, H.-Z. *Langmuir* **2005**, *21*, 5013−5018.
(31) Munford, M. L.; Cortès, R.; Allongue, P. *Sens. Mater.* **2001**, *13*, 259−269.
(32) Allongue, P.; Henry de Villeneuve, C.; Morin, S.; Boukherroub, R.; Wayner, D. D. M. *Electrochim. Acta* **2000**, *45*, 4591−4598.

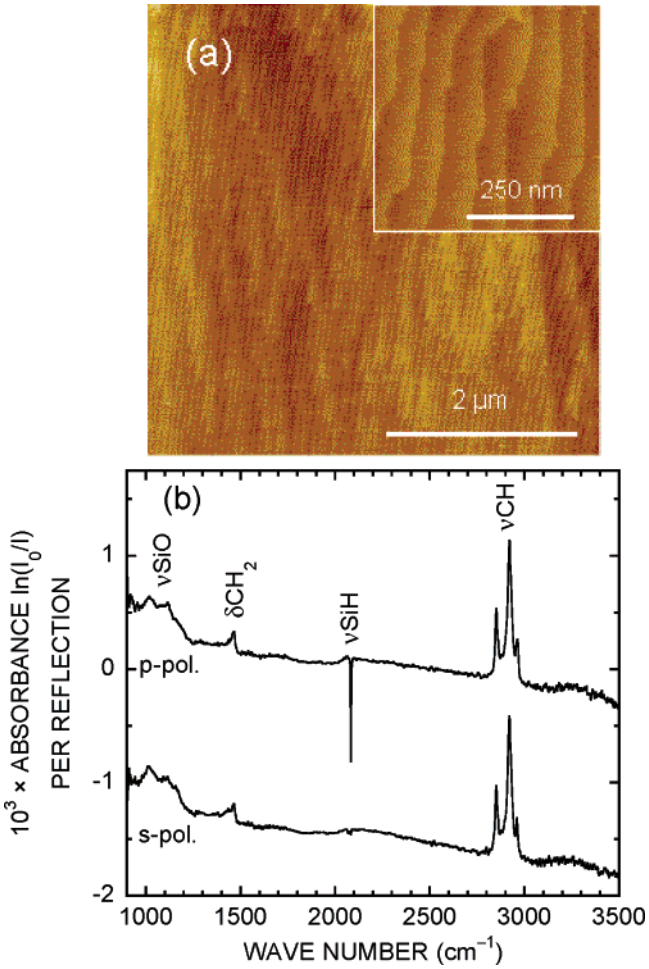

Figure 1. Si(111) surface modified with a decyl monolayer. (a) 5 μm × 5 μm AFM image; the inset (500 nm × 500 nm) shows better evidence of the (111) terraces separated by atomic steps. (b) Corresponding ATR-FTIR spectra recorded in s and p polarization (no baseline correction). The band assignments are as indicated.

on the hydrogen-terminated Si(111) surface. It was rinsed with tetrahydrofuran (THF) and dichloromethane (CH_2Cl_2) right after the reaction. The AFM topography is identical to that of a freshly etched H−Si(111) surface with atomically smooth terraces separated by atomic steps corresponding to one silicon bilayer (0.31 nm).[31] The short-range peak-to-peak roughness measured on one (111) terrace is ca. 0.1 nm, which is slightly larger than the corresponding measurement on a H-terminated surface. On such a surface, contact-mode AFM imaging causes no problem. In particular, prolonged tip scanning on a given location does not remove any adventitious organic material. There is also no image contrast in friction images. Hence, alkyl monolayers appear to be homogeneous on the nanometer scale and free of any contaminants. The IR spectra with s and p polarization display all of the expected vibrational bands. (See assignments in the Figure.) Note that the sharp negative peak at 2083 cm^{-1} is not observed in s polarization because it is related to Si−H bonds that are normal to the silicon (111) terraces. The fact that the Si−H-related peak is *negative* indicates a loss of H atoms from the surface in agreement with Scheme 1. The broad, low-intensity, positive peak around 2070 cm^{-1} superimposed on the sharp Si−H peak arises from a Si−H vibration modified by the presence of the organic layer.[33] This implies that the substitution is not complete, in agreement with the fact that 50% of the Si−H sites may, at most, be grafted.[34] The IR band associated with the Si−H remaining on the surface is broadened because of weak interactions between the Si−H vibrators and the neighboring molecular chains.[35−37] The weak, broad band in the region of 900−1200 cm^{-1} indicates the presence of some oxide on the surface, a common problem in hydrosilylation.[4] Our data suggest the formation of 0.1 equiv of the native-oxide layer in the form of nanometer-sized SiO_2 clusters[38] rather than the oxidation of the remaining SiH sites.[4] The CH band will be discussed in more detail below. This alkyl-terminated surface may therefore be considered to be a reference sample with a well-defined organic monolayer.

When transposing the above process to the preparation of 100% acid-terminated samples, we never observed a clean surface such as the one shown in Figure 1. The left-hand column of Figure 2 presents typical AFM images of 25 to 100% acid-terminated surfaces rinsed in THF and CH_2Cl_2, which is a procedure commonly used in the literature. Increasing the surface concentration of acid groups degrades the resolution of the silicon steps (compare images a and c); one simultaneously observes an increasing surface density of white spots. In addition, some meandering white lines are running across the surface. Hence, AFM imaging gives direct evidence that the tip sweeps some loose material across the surface (Figure 2a−c). A more controlled test consists of imaging the same region several times (without applying a large force) and then enlarging the scanned area. The 1 μm × 1 μm square box in image c was created in this way, which demonstrates that prolonged tip scanning is wiping unwanted materials atop the monolayer. After a while, the silicon steps become clearly visible (image d), meaning that the surface was locally cleaned by the AFM tip. Other aprotic solvents were used: 1,1,1-trichloroethane, acetone, and toluene did not give better results. Protic solvents (methanol and ethanol) were also tested without success. Sonification during rinsing was not found to improve surface cleanliness either. An optimal rinse was finally obtained in hot acetic acid (CH_3COOH). The AFM images displayed in the right-hand column of Figure 2 (images e−h) demonstrate that this procedure gives excellent results. Now the surface appears perfectly clean for any surface concentration of carboxyl groups. The Si(111) terraces are smooth on the atomic scale, and no material is removed by the tip even upon prolonged scanning. No significant contrast is observed in friction images. Properly rinsed acid-terminated monolayers are therefore homogeneous on the nanometer scale and free of any unwanted material.

Figure 3 compares the ATR-FTIR spectrum (p polarization) of a 100% acid-terminated surface rinsed in THF + CH_2Cl_2 (curve a) and in hot acetic acid (curve b). The two spectra exhibit the same expected IR bands. (See assignments in the Figure.)

(33) Fellah, S.; Teyssot, A.; Ozanam, F.; Chazalviel, J.-N.; Vigneron, J.; Etcheberry, A. *Langmuir* **2002**, *18*, 5851−5860.

(34) Sieval, A. B.; van den Hout, B.; Zuilhof, H.; Sudhölter, E. J. R. *Langmuir* **2001**, *17*, 2172−2181.

(35) Venkateswara Rao, A.; Ozanam, F.; Chazalviel, J.-N. *J. Electrochem. Soc*. **1991**, *138*, 153−159.

(36) Ozanam, F.; Djebri, A.; Chazalviel, J.-N. *Electrochim. Acta* **1996**, *41*, 687−692.

(37) Nakamura, M.; Song, M. B.; Ito, M. *Electrochim. Acta* **1996**, *41*, 681−686.

(38) From other observations (area concentration of grafted chains, survival of SiH bonds, and absence of SiH sites with oxidized back-bonds), we infer that the oxide is in the form of clusters. From the integrated intensity A of the bands related to silicon oxide in s polarization (0.068 cm^{-1} for Figure 1b when integrated over 900−1200 cm^{-1}), one can estimate an equivalent oxide thickness of $\Delta = n_1 A \cos\theta/(\pi^2 I_y C)$ (where $n_1 = 3.42$, $\theta = 45°$, $I_y = 2.19$, and $C = 0.88\ 10^6\ cm^{-2}$) (See Appendix in Chazalviel, J.-N.; da Fonseca, C.; Ozanam, F. *J. Electrochem. Soc*. **1998**, *145*, 964−973). Hence, $\Delta/A = 12.7$ Å/(cm^{-1}) by treating the oxide as bulk silica. Under this assumption, an equivalent SiO_2 thickness of 0.9 Å is found. This may be accounted for by clusters with the following characteristics: height 1 nm, diameter 3 nm, density $10^{12}\ cm^{-2}$. Such characteristics make the nanometer clusters hardly resolved by AFM because of the finite size of the AFM tip.

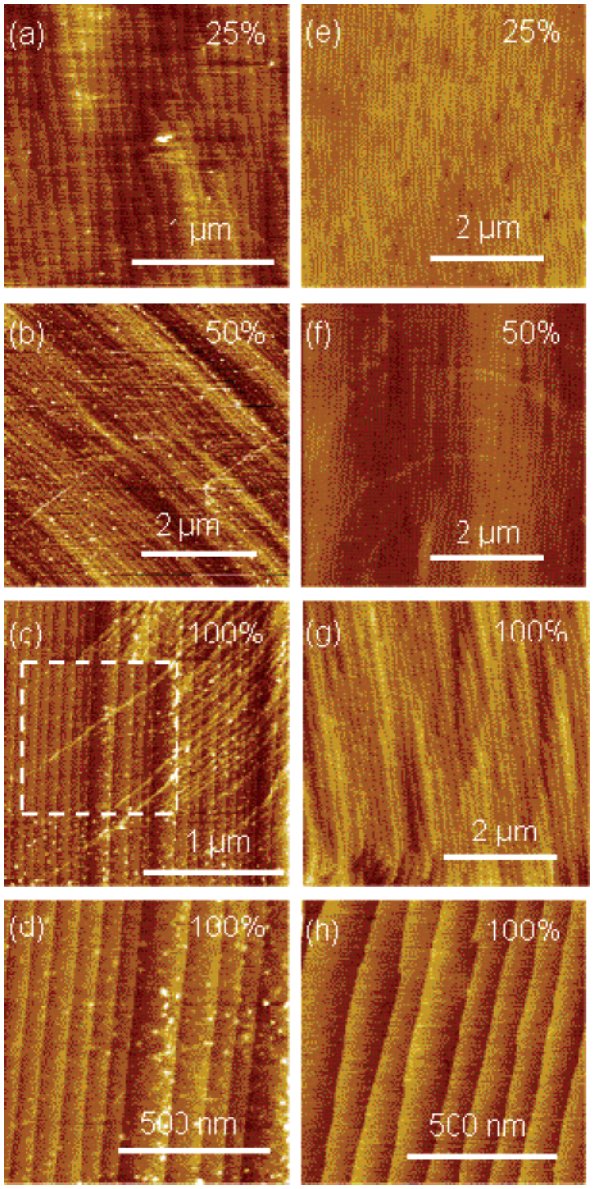

Figure 2. Contact mode AFM images of Si(111) surfaces modified by direct functionalization with mixed acid- and methyl-terminated alkyl monolayers. The volume fraction of undecylenic acid in the grafting solution is indicated in the images. Left-hand column: samples rinsed with hot CH_2Cl_2 and TCE (see text). Right-hand column: samples rinsed with hot CH_3COOH.

The characteristics of the sharp negative peak assigned to Si−H are identical to those noticed for the alkyl-terminated surface (Figure 1). One also notices that the IR bands related to SiO_2 (1000−1200 cm^{-1} region) are largely suppressed. This suggests that the oxide found after grafting in 1-decene stems from residual water, which is trapped by undecylenic acid. The different CH bands in the range of 2840−2980 cm^{-1} will be discussed in more detail later. The band at 1467 cm^{-1} is assigned to the CH_2 scissor mode of the methylene groups. The peak at 1715 cm^{-1} is consistent with the C═O stretching mode of hydrogen-bonded carboxylic acids.[39,40] The clear observation of the C−O−H in-plane modes (1289 and 1410 cm^{-1}) means that the acid end groups are left intact after the reaction. Finally, the weakness of the band around 1100 cm^{-1} indicates a very low concentration

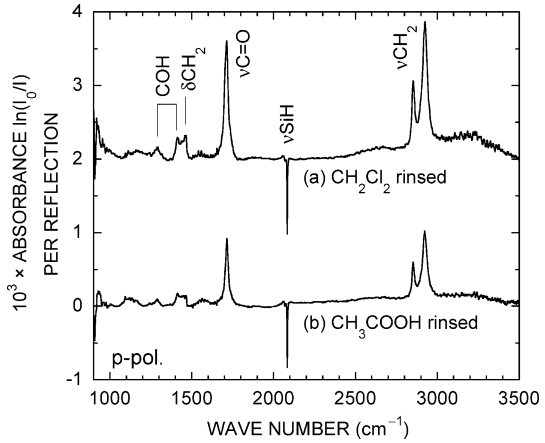

Figure 3. ATR-IR spectra (p polarization) of a 100% carboxydecyl-terminated surface. (a) Sample rinsed in THF and CH_2Cl_2. (b) Sample rinsed in hot acetic acid. A different sample was used in each case. Note that the intensity of the CH and C═O related IR bands is divided by a factor of ∼2 in the case of the CH_3COOH rinse, whereas the intensity of the Si−H band remains unchanged within ∼10%.

of Si−O−Si and Si−O−C groups. A quantitative analysis of this band sets an upper bound of 0.1 Å for the effective SiO_2 thickness (if the band is entirely attributed to Si−O−Si) or ∼5 × 10^{13} cm^{-2} for the surface concentration of siloxane esters groups Si−O−CO (if the band is entirely attributed to Si−O−C). The shape of the band makes its attribution to SiO_2 more plausible, which points to a surface concentration of Si−O−C groups at most on the order of a few percent of that of grafted acid chains. The spectra in Figure 3 are therefore clear-cut proof that grafting via the carbonyl end groups during the surface modification is negligible and the interface is essentially oxide free.

A quantitative inspection of the spectra reveals that the integrated intensity of the CH- and COOH-related IR bands is divided by a factor of ∼2 if the surface is rinsed in acetic acid (curve b) instead of THF and CH_2Cl_2 (curve a). This indicates that the former procedure removes molecules that are physisorbed on the surface after the grafting reaction, in close agreement with the AFM observations (Figure 2). The observed variation in the Si−H peak intensity (∼10% at 2083 cm^{-1}) can be ascribed to the accuracy of data analysis (e.g., for determining the number of reflections) because two different prisms were used for the two rinsing protocols. It is much smaller than that of the CH and COOH peaks. This suggests the formation of a molecular bilayer during the reaction (Figure 4), which is consistent with the known strength of hydrogen bonding in carboxylic acid dimers (ΔH = 15 $kcalmol^{-1}$).[41,42] The fact that the C═C double bonds of unreacted undecylenic acid (∼1640 cm^{-1}) are not resolved in Figure 3 (spectrum a) is attributed to their weak IR cross section. The associated IR intensity is indeed estimated to be only ∼1.5% of that of the CO stretching mode, which is below the detection limit. Because the CO and CH absorbances are divided by the *same* factor of 2 upon rinsing in hot acetic acid, we infer that acetic acid has the capability of breaking the hydrogen bonds by displacing the unreacted undecylenic acid molecules and desorbing from the surface upon drying. It was confirmed that another rinse with water, which is miscible with acetic acid and is able to break hydrogen bonds,[43,44] leaves the intensity of the IR bands

(39) Arnold, R.; Azzam, W.; Terfort, A.; Wöll, C. *Langmuir* **2002**, *18*, 3980−3992.
(40) Willey, T. M.; Vance, A. L.; van Buuren, T.; Bostedt, C.; Nelson, A. J.; Terminello, L. J.; Fadley, C. S. *Langmuir* **2004**, *20*, 2746−2752.
(41) Schuster, P. In *The Hydrogen Bond*; Schuster, P., Zundel, G., Sandorfy, C., Eds.; North-Holland: Amsterdam, 1976; p 117.
(42) Steiner, T. *Angew. Chem., Int. Ed.* **2002**, *41*, 48−76.
(43) Stahl, N.; Jencks, W. P. *J. Am. Chem. Soc.* **1986**, *108*, 4196−4205.
(44) March, J. *Advanced Organic Chemistry*, 4th ed.; Wiley: New York, 1992; p 76.

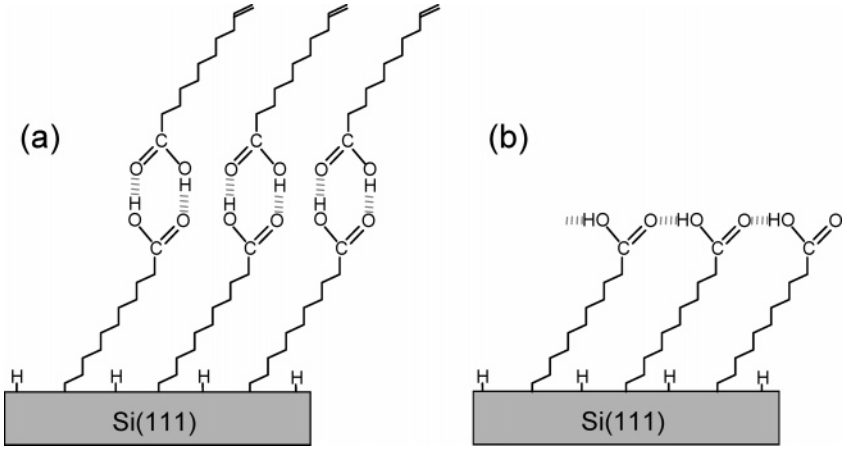

Figure 4. Scheme of the acid-modified surface (a) after a conventional rinse with CH_2Cl_2 and (b) after a proper rinse with CH_3COOH.

Table 1. Summary of the IR Absorption Frequencies of the CH_3, CH_2, and C=O Stretching Modes and Their Integrated Absorbances for 100% Decyl, Mixed 10-Carboxydecyl/Decyl, and 100% Carboxydecyl Monolayers

	frequency in cm^{-1} (area)			
% COOH[a]	ν_aCH_3	ν_aCH_2	ν_sCH_2	νCO
0	2962.3 (0.0049)[b]	2921.7 (0.049)[b]	2851.9 (0.0128; 0.0134)[c]	
25	2960.0 (0.0022)	2921.0 (0.048)	2850.8 (0.0131; 0.0136)	1715.6 (0.0127; 0.0116)
50	2961.7 (0.0018)	2922.3 (0.053)	2851.6 (0.0115; 0.0111)	1715.1 (0.0221; 0.0196)
100		2923.9 (0.045)	2853.0 (0.0116; 0.0116)	1714.6 (0.0302; 0.0276)

[a] Indicates the undecylenic acid proportion in the reaction mixture. The area values of the ν_sCH_2 and νCO modes are given with a 5% error margin, and those of ν_aCH_2, with a 10% error margin. [b] p polarization. [c] p polarization; s polarization.

related to CO unchanged. In other words, no CH_3COOH molecules were removed. Therefore, we conclude that a 100% acid-terminated silicon surface prepared by hydrosilylation of ω-alkenoic acids and properly rinsed in acetic acid is well defined on the molecular scale. In particular, it is free of physisorbed undecylenic acid and acetic acid molecules.

3.2. Quantitative Determination of the Molecular Surface Concentrations. The position of asymmetric stretching mode ν_aCH_2 is generally used to qualitatively assess the packing of alkyl chains on silicon. A monolayer is considered to be compact when the frequency of this mode decreases and approaches that of the corresponding crystalline material (2917 cm^{-1}).[45,46] This criterion remains qualitative, and as mentioned above, it is highly desirable to obtain an independent and, better, a *quantitative* determination of the molecular surface concentration. This section describes the quantitative analysis of FTIR spectra using calibration experiments. Details of the calibration procedure are given in the Appendix.

In the case of mixed acid-terminated monolayers, the infrared spectra are complicated: four CH modes are expected from symmetry considerations, which are superimposed on other contributions enhanced by Fermi resonance.[47,48] The νCH stretching vibrations were therefore fitted by using a model consisting of a linear baseline and the superimposition of five Voigt functions representing the four CH_2 and CH_3 modes and the main Fermi-resonance-enhanced contribution at ~2900 cm^{-1}. Such a procedure has been proven to be very robust. In particular, the intensity of the ν_sCH_2 mode (~2850 cm^{-1}) is only weakly sensitive to the other fitting parameters. The frequency and integrated intensities of the three most salient νCH modes (symmetric (ν_s) CH_2, antisymmetric (ν_a) CH_2, and CH_3 stretching modes) are listed in Table 1. The νCO mode was similarly fitted by using a single Lorentzian profile. The intensity of the CO stretching mode is also given in Table 1. As expected, the results show that the intensity of the carbonyl band decreases with decreasing volume concentration of acid in the grafting solution whereas that of the antisymmetric CH_3 stretching band (2961 cm^{-1}) somewhat increases. Another clear trend is the increase in the (ν_a) CH_2 frequency with increasing acid-chain surface concentration. This indicates a decrease in layer density probably because of the fact that the carboxyl terminal group is bulkier than the methyl group.

The intensity values listed in Table 1 were converted into absolute numbers of CH_2 and COOH groups using calibration FTIR experiments explained in detail in the Appendix (eqs A9 and A10). As justified in the Appendix, the intensity of the symmetric ν_sCH_2 mode (~2850 cm^{-1}) was used to estimate the *total* surface density of CH_2 groups. The infrared cross section of the ν_sCH_2 mode was extracted from a calibration experiment in dodecane. Briefly, the νCH band of the solution is fitted as described above, and the absorbance per CH_2 group was determined taking into account the penetration depth of the infrared radiation inside liquid dodecane. The infrared cross section of the νCO mode is similarly extracted from a calibration experiment using a solution of 1% decanoic acid in dodecane (v/v). A dilute solution was used to avoid variations of the refractive index in the νCO spectral range.

The CH calibration allows for the determination of the *total* area density of methylene groups on the surface. This includes those methylene groups on the acid-terminated decyl chains and those on the decyl chains. The CO calibration allows for the direct determination of the absolute area density of the acid chains immobilized on the surface. From the result, we derived the density of alkyl chains accounting for the fact that there are 10 methylene groups per acid chain and 9 per alkyl chain. The

(45) Snyder, R. G.; Strauss, H. L.; Elliger, C. A. *J. Phys. Chem.* **1982**, *86*, 5145−5150.
(46) Porter, M. D.; Bright, T. B.; Allara, D. L.; Chidsey, C. E. D. *J. Am. Chem. Soc.* **1987**, *109*, 3559−3568.
(47) Nuzzo, R. G.; Dubois, L. H.; Allara, D. L. *J. Am. Chem. Soc.* **1990**, *112*, 558−569.
(48) Ward, R. N.; Duffy, D. C.; Davies, P. B.; Bain, C. D. *J. Phys. Chem.* **1994**, *98*, 8536−8542.

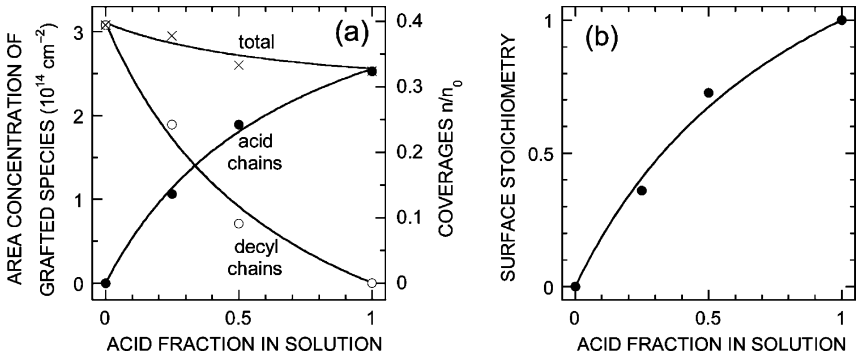

Figure 5. Composition of monolayers grafted from carboxydecyl/decyl mixtures. (a) Area concentration of the decyl (○) and carboxydecyl chains (●) and total concentration (×) as a function of the undecylenic acid fraction in the grafting solution. The corresponding coverages are given by the right-hand-side vertical scale. The points are experimental data, and the solid curves are the fits according to eqs 4−6. (b) Acid-chain surface stoichiometry derived from part a, fitted with eq 7.

surface density of acid-terminated chains and decyl chains and the *total* density of molecular chains are plotted in Figure 5a as a function of the undecylenic acid volume concentration in the grafting solution. The corresponding surface coverages θ are found from the right-hand scale in Figure 5a. They were computed as the ratios of the corresponding densities of grafted chains to the surface density of Si−H bonds on the hydrogenated Si(111) surface (7.83×10^{14} cm^{-2}). The total coverage indicates that all of the monolayers are fairly dense, with $0.32 < \theta < 0.39$, remembering that the maximum attainable surface coverage is ~50% on Si(111).[34] One also notices that the total surface density significantly decreases with increasing acid content, which gives credit to the qualitative conclusion derived above from the ν_a-CH_2 mode frequency shift toward greater wavenumbers. A plausible reason is steric hindrance by the bulky COOH end groups. The nonlinear variation of the surface concentration of acid chains indicates that the mixed monolayers are *richer* in acid chains than the grafting solution. This point will be discussed in detail in the next section.

3.3. Composition of the Mixed Monolayers. As noticed above, the area concentrations of acid (●) and alkyl (○) chains grafted onto the surface exhibit a nonlinear relationship as a function of the composition of the grafting solution (Figure 5), indicating an enrichment in acid chain in the monolayer. A more direct indication of this effect is given by Figure 5b, showing the stoichiometry of the grafted layer as a function of solution stoichiometry. These results stand in contrast to the linear variations found for mixed ethoxycarbonyl-alkyl/alkyl monolayers.[21,26]

This result can be rationalized in terms of first-order grafting kinetics if different rate constants are taken for the two species

$$\frac{dn_1}{dt} = k_1c_1(n_0 - a_1n_1 - a_2n_2) \text{ and } \frac{dn_2}{dt} = k_2c_2(n_0 - a_1n_1 - a_2n_2) \quad (1)$$

where the indexes 1 and 2 refer to 1-decene and undecylenic acid, respectively. n, c, k, and a represent the respective area concentration, fraction in the liquid ($c_1 + c_2 = 1$), rate constant, and mean number of surface sites blocked by one grafted chain. Parameters a_1 and a_2 are necessary to account for a maximum coverage lower than 1: a represents the occupancy of a grafted site plus the hindered next neighboring sites and is plausibly a number on the order of 2 because the maximum coverage is ~0.5 for an ideally packed monolayer. n_0 is the total area density of surface sites ($n_0 = 7.83 \times 10^{14}$ cm^{-2}) and $n_0 - a_1n_1 - a_2n_2$ is the area density of sites available for grafting at time t. Full modification is reached when $a_1n_1 + a_2n_2 = n_0$. Combining the two equations leads to

$$\frac{d(a_1n_1 + a_2n_2)}{dt} = (k_1a_1c_1 + k_2a_2c_2)[n_0 - (a_1n_1 + a_2n_2)] \quad (2)$$

which can readily be integrated with the initial conditions $n_1 = n_2 = 0$ at $t = 0$:

$$a_1n_1 + a_2n_2 = n_0\{1 - \exp[-(k_1a_1c_1 + k_2a_2c_2)t]\} \quad (3)$$

By substituting eq 3 into the second members of eq 1, functions $n_1(t)$ and $n_2(t)$ are obtained, leading to the steady state (infinite t):

$$n_1 = n_0\frac{k_1c_1}{k_1a_1c_1 + k_2a_2c_2} = n_0\frac{1 - c_2}{a_1 + [(k_2/k_1)a_2 - a_1]c_2} \quad (4)$$

and

$$n_2 = n_0\frac{k_2c_2}{k_1a_1c_1 + k_2a_2c_2} = n_0\frac{(k_2/k_1)c_2}{a_1 + [(k_2/k_1)a_2 - a_1]c_2} \quad (5)$$

Hence,

$$n_1 + n_2 = n_0\frac{k_1c_1 + k_2c_2}{k_1a_1c_1 + k_2a_2c_2} = n_0\frac{1 + [(k_2/k_1) - 1]c_2}{a_1 + [(k_2/k_1)a_2 - a_1]c_2} \quad (6)$$

and

$$\frac{n_2}{n_1 + n_2} = \frac{k_2c_2}{k_1c_1 + k_2c_2} = \frac{(k_2/k_1)c_2}{1 + [(k_2/k_1) - 1]c_2} \quad (7)$$

The data in Figure 5a are consistent with eqs 4−6, with $a_1 = 2.52$, $a_2 = 3.06$, and $k_2/k_1 = 1.98$ (solid curves in Figure 5a). The greater value of a found for acid chains means, as anticipated, that the COOH terminal group is bulkier than the methyl terminal group. Note however that parameters a_1 and a_2 play a minor role in the above analysis. (Their value is essentially determined by the area concentrations for $c_2 = 0$ and $c_2 = 1$.) As a matter of fact, the fit is mostly dependent on parameter k_2/k_1. In a simpler approach, one may limit the analysis to the fit of the plot in Figure 5b using eq 7, which depends on k_2/k_1 only. The resulting value $k_2/k_1 = 2.07$ is in fair agreement with the above value of 1.98, which confirms the robustness of the fit and indicates a faster reaction kinetics of the undecylenic acid molecules as compared to that of 1-decene (about twice as fast). A plausible

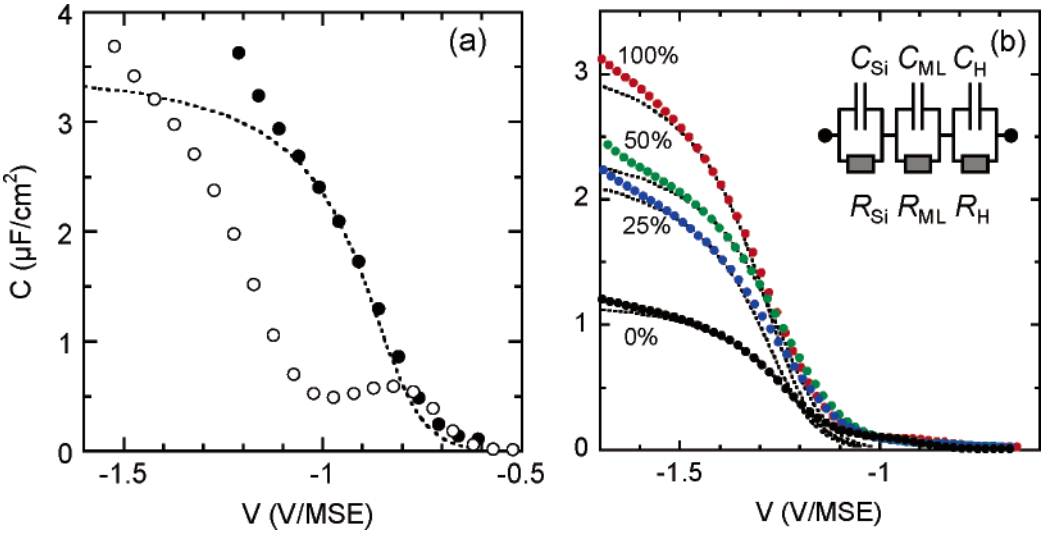

Figure 6. Capacitance−potential curves recorded at 9 kHz in 0.1 M H_2SO_4 with different n-type Si(111) electrodes. (a) H−Si(111) (●) and oxidized (○) surfaces. (b) Si(111) surface modified photochemically with mixed acid monolayers. The volume fraction of undecylenic acid in 1-decene is indicated. Note that all plots have a monotonic rise, except for the oxidized surface in part a, which exhibits a capacitance peak. Points (●, ○) are experimental data, and the dotted curves are calculated.

interpretation is that the acid functional groups favor physisorption of the acid as compared to the alkene, which leads to a higher grafting probability.

3.4. Electronic Properties of the Silicon−Acid Monolayer Interface. Electrochemical capacitance measurements provide a straightforward approach to examine the electronic properties of the silicon/electrolyte interface as well as the dielectric properties of the organic films.[49,50] The impedance of the semiconductor/electrolyte interface may be modeled by the series combination of different parallel *RC* elements (inset of Figure 6b), standing for electron transfer across the space charge region in silicon (R_{Si}, C_{Si}), the molecular layer (R_{ML}, C_{ML}), and the electrochemical double layer (R_H, C_H). At sufficiently high frequency, the impedance becomes equivalent to the series combination of the above-defined capacitances. For all of our data, the imaginary part of the impedance was indeed found to be equivalent to a (frequency-independent) capacitance in the range of 1−10 kHz.

The only bias-dependent capacitance is C_{Si}, which in the accumulation regime can be written as[49] $C_{Si} = \sqrt{\frac{q^2\epsilon_{Si}\epsilon_0 N_D}{kT}}\exp(-q[(V - V_{fb})/2kT])$ within the classical Poisson−Boltzmann approximation. In this expression, V_{fb} is the flat band potential of silicon, and all other symbols have their usual meaning. Though this expression overestimates C_{Si}, we have verified that the whole procedure is not significantly affected by this problem.[51] The procedure for the curve simulation has been described in ref 49. In practice, the value of C_H is first determined at the H-terminated surface, and we assume that the same value stands for the modified samples. The value of the interface capacitance at the modified sample yields the monolayer capacitance $C_{ML} = [\epsilon_{eff}\epsilon_0/\delta]$, where ϵ_{eff} is the *effective* dielectric constant of the organic film. As explained elsewhere,[49] Bruggeman effective medium theory can be used to derive the volume fraction F occupied by the molecules, assuming that the organic film is composed of molecules and water inclusions. More details are given elsewhere.[49] It is important to recall that the curve simulation assumes that no electronic states are present at the silicon surface.

The capacitance−voltage characteristics of a H-terminated (●) and of an oxidized (○) n-type Si(111) electrode are given in Figure 6a. The general shape is monotonic with a saturation plateau toward negative potentials. An additional capacitance peak (between −1 and −0.6 V) is observed for the oxidized electrode. The line in Figure 6a is a calculated $C-V$ curve with $C_H = 3.5\ \mu F\ cm^{-2}$ and a flat band potential of −0.7 V for the H-terminated sample. (V_{fb} coincides with the rise in the capacitance toward negative potentials.) The good agreement between the experimental data and the calculation, if one excludes the potential range where a Faradaic process takes place, is consistent with the fact that the H-terminated Si(111) surface presents a very low density of surface states.[52] In the case of the oxidized surface, the pronounced capacitance peak is attributed to charge relaxation processes between the conduction band and surface states. The flat band potential is correspondingly shifted to −1 V because of the accumulation of additional charges at negative potential. Figure 6b presents the capacitance−voltage characteristics of mixed acid-terminated silicon (111) surfaces. The shape of the curves is indicative of a low density of interface states, by analogy to the case of a bare surface, and one also notices that the flat band potential is shifted with respect to the hydrogenated surface. This is a result of the efficient protection of the surface by the grafted layer.[53] Moreover, the flat band potential is essentially independent of the acid-chain surface concentration, indicating that the dipole associated with the carboxyl group is either nearly parallel to the interface plane or screened by the electrolyte. These observations are consistent with the fact that no surface oxidation was detected from FTIR (Figure 3).

Focusing on the saturation plateaus in Figure 6b, where the measurement becomes almost insensitive to C_{Si} because $C_{Si} \gg C_{ML}$ and C_H, the present observations seem, to a first approximation, consistent with expectations because the saturation capacitance decreases after the organic modification of the surface.

(49) Allongue, P.; Henry de Villeneuve, C.; Pinson, J. *Electrochim. Acta* **2000**, *45*, 3241−3248.
(50) Yu, H.-Z.; Morin, S.; Wayner, D. D. M.; Allongue, P.; Henry de Villeneuve, C. *J. Phys. Chem. B* **2000**, *104*, 11157−11161.
(51) Allongue, P.; Henry de Villeneuve, C.; Ozanam, F.; Chazalviel, J.-N. Unpublished results.
(52) Yablonovitch, E.; Allara, D. L.; Chang, C. C.; Gmitter, T.; Bright, T. B. *Phys. Rev. Lett.* **1986**, *57*, 249−252.
(53) Henry de Villeneuve, C.; Gorostiza, P.; Sanz, F.; Sun, Q. Y.; Boukherroub, R.; Allongue, P. To be submitted for publication.

Table 2. Electrochemical Characterizations (OCP, Flat Band Potential) and Dielectric Constant of Monolayers Derived from the *C*(*V*) Curves of Figure 6b[a]

% COOH (solution)	% COOH (surf)	V_{fb} V/MSE	C_{MH} μF cm^{-2}	C_{ML}[b] μFcm^{-2}	ϵ_{eff}[c]	coverage[d] θ
0	0	−1.105	1.31	2.09	2.7	0.47
25	36	−1.099	2.36	7.25	9.3	0.34
50	73	−1.142	2.55	9.39	12.1	0.32
100	100	−1.088	3.31	61.0	78.5	0.01

[a] The surface coverage was calculated as explained in the text using effective medium theory. [b] Calculated for $C_H = 3.5\,\mu$F cm^{-2} [c] Calculated from C_{ML} with $\delta = 1.14$ nm. [d] Taken as $F/2$, where F is calculated from $\epsilon_{mol} = 2.3$ and $\epsilon_{sol} = 80$.

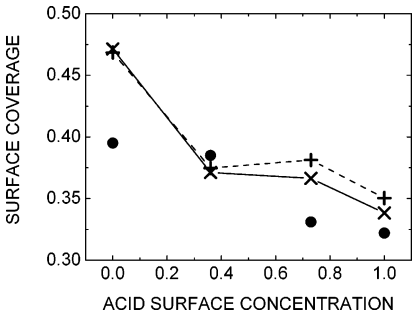

Figure 7. Surface coverage of mixed acid monolayers as a function of the acid-chain surface stoichiometry. (●) Experimental data derived from IR (Figure 5); (×) coverage calculated from effective medium theory using $C_H = 3.5\,\mu$F cm^{-2} and ϵ_{sol} infinite; (+) the same but calculated with C_H a linear function of θ_2 and $\epsilon_{sol} = 80$. See the text for more details.

Assuming an equal δ layer thickness for alkyl- and acid-terminated monolayers, ϵ_{eff} was calculated from C_{ML}. Table 2 lists the ϵ_{eff} values calculated using $C_H = 3.5\,\mu$F cm^{-2} and $\delta = 1.14$ nm. (We assume that the chains are tilted by 35° with respect to the surface normal and that the layer thickness is equal to the chain length projected on the surface normal.) The value $\epsilon_{eff} = 2.7$ found for the alkyl monolayer is comparable to that of polyethylene ($\epsilon = 2.3$) and means that the organic film is dense in agreement with FTIR (Figure 5). The mixed monolayers present larger ϵ_{eff} values. Using effective medium theory with $\epsilon_{mol} = 2.3$ (dielectric constant of polyethylene) and $\epsilon_{sol} = 80$ (water), we calculated the volume fraction F of molecules in the organic film and the corresponding surface coverage $\theta = F/2$ ($F = 1$ roughly corresponds to $\theta = 0.5$, see above). There is a fair agreement between this analysis and the IR results for mixed monolayers of intermediate acid content and for the alkyl monolayer (compare Table 2, last column and Figure 5). However, this analysis totally fails for the 100% acid-terminated sample, with a calculated $\theta \approx 0$, although IR spectroscopy proved that the surface coverage is $\theta = 0.32$.

The above discrepancy calls for a necessary adaptation of the present model. Two hypotheses may be envisioned. The first hypothesis would be to consider that the organic molecular layer is permeable not only to molecular water, as assumed above, but also to ionic species. This amounts to considering that the monolayer is a mixture of organic chains ($\epsilon_{mol} = 2.3$) and a conducting electrolyte (ϵ_{Sol} infinite). Computing again $\theta = F_\infty/2$, where F_∞ is the fraction of molecules calculated with ϵ_{Sol} infinite, we now find values that are in agreement with those determined by IR spectroscopy over the whole range of acid-chain surface concentration. (Compare the -×- plot with ● in Figure 7.) The alternate hypothesis is to assume that the Helmholtz capacitance C_H depends on the chemical termination of the monolayer. The acid-terminated surface is indeed highly hydrophilic whereas the methyl-terminated and the H−Si(111) surfaces are highly hydrophobic surfaces. This is likely to affect

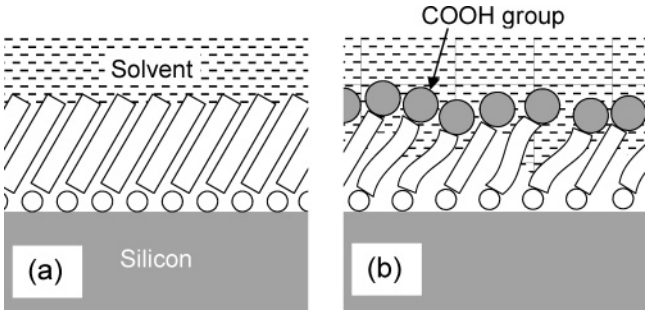

Figure 8. Schematic representation of the different penetration depths of the solvent into an alkyl monolayer (a) and into an acid-terminated monolayer (b). Note that water does not reach the silicon surface in part b.

the structure of water close to the interface as well as the water dipole orientation. Significant differences in the double-layer structure were indeed observed in the case of self-assembled monolayers of hydroxythiol and alkanethiols on Au(111).[54] Tentatively assuming that C_H increases at the carboxyl-terminated monolayer, it is sufficient to consider $C_H = C_H^{COOH} = 7\,\mu$F cm^{-2} at the 100% acid-terminated surface to reduce the ϵ_{eff} value drastically from 78.5 to a more realistic value of 8.2. Writing that $C_H = (1 - \theta_2)C_H^{CH_3} + \theta_2 C_H^{COOH}$ at mixed monolayers and converting the ϵ_{eff} values found into a surface coverage (see above) with $\epsilon_{Sol} = 80$ and $\epsilon_{Mol} = 2.3$ gives the plot in Figure 7 (-+-). The agreement with the IR data is again good over the entire range of acid-chain surface stoichiometry.

Though it is as yet difficult to decide between these two hypotheses, they both mean that the penetration of the solvent is much more prominent at mixed acid monolayers (Figure 8b) than at decyl monolayers (Figure 8a). However, it seems clear that the liquid *is not yet touching* the silicon surface because the quite negative value of the flat band potential measured at the modified surfaces, as compared to that at the H−Si(111) surface (Table 2), indicates that the silicon surface remains isolated from the electrolyte.[53] The above analyses both give a volume fraction of molecules of about $^2/_3$ for all acid-terminated monolayers, which is close to the percolation threshold within the Bruggeman approximation, whereas the alkyl monolayer is denser. Hence, a possible interpretation is that the smaller surface coverage of the acid-terminated monolayers allows for larger fluctuations in the *local* molecular density, thereby opening wider gaps for water penetration into the inner, hydrophobic part of the layer. Also, the hydrophilic carboxyl groups may favor water penetration in their vicinity, that is, in the outer part of the layer, including regions that would (if alone) be hydrophobic.

4. Conclusions

We have demonstrated that *direct* photochemical reaction of undecylenic acid on the hydrogenated Si(111) surface leads to monolayers terminated with intact carboxylic acid end groups. The IR spectra prove that no reaction occurs between the carboxyl group and the silicon surface. In addition, the interface remains oxide-free. A well-defined modified surface, free of unwanted materials, is obtained only upon rinsing in hot acetic acid. Other solvents leave physisorbed unreacted undecylenic chains as found from AFM imaging and the intensity of the CH and C═O IR bands, which is a piece of information that may account for some controversial results in the literature. A *quantitative* analysis of the IR spectra indicates that the mixed acid monolayers are quite dense with a surface coverage increasing from 0.32 to 0.39 as

(54) Becka, A. M.; Miller, C. J. *J. Phys. Chem.* **1993**, *97*, 6233−6239.

the acid-chain surface concentration decreases from 100 to 0%. Because of a faster reaction kinetics with undecylenic acid, mixed carboxydecyl/decyl monolayers are richer in acid chains than the grafting solution. While the absence of interfacial oxide preserves a low density of states at the modified surface, as evidenced from impedance measurements, the effective dielectric constant increases remarkably with increasing acid content, indicating that water penetration inside the organic film is promoted by the carboxyl-terminal groups. The solvent, however, remains in the outer part of the organic film and does not reach the silicon surface.

Appendix: Calibration of the IR Absorption Intensity of Adsorbates

In ATR geometry, the intensity of the signal associated with the infrared vibrational mode of an adsorbate can easily be computed, provided that the infrared cross section of the mode is known. As shown hereafter, this cross section can be simply determined if the absorption of the considered mode can be measured in a liquid-phase experiment in the same geometry.

In an assembly of molecules, a convenient way is to adopt a macroscopic description and consider the dielectric response of this assembly. In this approach, all of the relevant microscopic details (such as the dynamic dipole of the considered vibrational mode) are included in an effective dielectric function, which, in the wavenumber range of interest, will be assumed to be simply related to the dielectric function of the liquid used for the calibration. An adsorbate layer may then be regarded as a slice of thickness δ and effective dielectric function $\epsilon = \epsilon' + i\epsilon''$ at the interface between a solid of refractive index n_s and a nonabsorbing medium of refractive index n_2. Following Chabal,[55] one may write its absorbance (i.e., the relative loss $\Delta I/I$ per reflection at wavelength λ in the infrared s- and p-polarized signals due to the presence of the layer)

$$a_s = \frac{2\pi}{\lambda}\frac{1}{n_s \cos\varphi} I_y \epsilon''_y \delta \tag{A1}$$

$$a_p = \frac{2\pi}{\lambda}\frac{1}{n_s \cos\varphi}\left(I_x \epsilon''_x \delta + I_z \frac{n_2^4}{\epsilon'^2_z + \epsilon''^2_z}\epsilon''_z \delta\right) \tag{A2}$$

where φ is the angle of incidence and I_x, I_y, and I_z numerical coefficients depending on n_s, n_2, and φ only.[55] For $n_s = 3.42$ (silicon), $n_2 = 1$ (air), and $\varphi = 45°$, $I_x = 1.98$, $I_y = 2.19$, and $I_z = 2.39$. Note that ϵ has been considered to be a tensor (with the z direction perpendicular to the interface plane) to possibly account for anisotropic effects due to the adsorbate configuration. With respect to this possibility, it is useful to consider the surface concentration of vibrators corresponding to the projection of the dynamic dipole of the vibrational mode in the interface plane, $N_{||}$, and that corresponding to the projection of the dynamic dipole along the z direction, $N_\perp$. Because the infrared signal is proportional to the square of the dynamic dipole ($N_\perp$ actually stands for $\sum_i \cos^2\theta_i$ and $N_{||}$ for $\sum_i \sin^2\theta_i$, where the sums run over the individual dipoles sitting on a unit surface area and θ_i represents the angle of dipole i with the surface normal), the actual surface concentration of vibrators is simply given by $N = N_{||} + N_\perp$.

In the calibration experiments, the infrared absorption of the liquid is measured in an attenuated total reflection configuration at the interface between the same solid and the liquid of complex refractive index $\tilde{n} = n_l + ik$. We suppose that k is small enough to neglect the change in the depth d of the evanescent wave due to absorption. In this case, the liquid absorbance (per reflection) is written as (in s and p polarization, respectively)

$$a'_s = \frac{2\pi}{\lambda}\frac{1}{n_s \cos\varphi} I'_y \, 2n_l k\frac{d}{2} \tag{A3}$$

$$a'_p = \frac{2\pi}{\lambda}\frac{1}{n_s \cos\varphi}(I'_x + I'_z) 2n_l k\frac{d}{2} \tag{A4}$$

where I'_x, I'_y, and I'_z are the same numerical coefficients as above, but with the values corresponding to n_l instead of n_2 ($I'_x = 1.91$, $I'_y = 2.42$, and $I'_z = 2.92$ with $n_l = 1.42$ for dodecane).

To obtain the sought calibration, assumptions have to be made to relate ϵ to $\tilde{n}$. We will therefore assume that (i) in the adsorbate layer, the absorption coefficient of the considered mode is proportional to the vibrator concentration in the layer with *the same proportionality coefficient* as that between the absorption coefficient and the vibrator concentration in the liquid and (ii) the real dielectric response of the adsorbate layer is isotropic and identical to that of the liquid (i.e., $n_l \approx \sqrt{\epsilon'_x} \approx \sqrt{\epsilon'_y} \approx \sqrt{\epsilon'_z}$. Physically, these assumptions mean only that the liquid mimics the same environment for the vibrators as that provided by the adsorbate layer. Denoting the concentration of vibrators in the liquid by C, the above assumptions yield

$$\frac{N_\perp/\delta}{C/3} = \frac{\epsilon''_z}{2kn_l} \tag{A5}$$

with the factor of $^1/_3$ accounting for the random orientation of the vibrators in the liquid. For simplicity, we will also consider that there is no anisotropy in the vibrational absorption of the layer in the interfacial plane (i.e., $\epsilon''_x = \epsilon''_y$, an assumption that could be avoided by considering two quantities N_x and N_y instead of $N_{||}$ defined above, but in this case, the determination of these two quantities would require an extra measurement.) We obtain similarly

$$\frac{N_{||}/2\delta}{C/3} = \frac{\epsilon''_x}{2kn_l} = \frac{\epsilon''_y}{2kn_l} \tag{A6}$$

It is then straightforward to derive $N_{||}$ from the ratio between the absorbance of the adsorbate layer and that measured for the liquid in s polarization:

$$N_{||} = \frac{a_s}{a'_s}\frac{I'_y}{I_y}\frac{C}{3}d \tag{A7}$$

Similarly, after simple algebra and considering that $\epsilon'^2_z + \epsilon''^2_z \approx \epsilon'^2_z$, one obtains $N_\perp$

$$N_\perp = \frac{I_y a_p - I_x a_s}{I_z a'_s/n_l^4}\frac{I'_y}{I_y}\frac{C}{3}\frac{d}{2} \tag{A8}$$

The above expressions rest on eqs A1−A3, that is, on absorbances measured at wavelength λ. However, because of the resonant character of the vibrational absorption and the weak wavelength dependence of all of the coefficients involved in eqs A1−A3, the same expressions will hold for absorbances integrated over a narrow wavenumber range around the vibrational resonance. Therefore, eqs A7 and A8 are used in practice for integrated absorbances because for a given mode the integrated absorbance is more reliably extracted from experimental data than the intrinsic spectral shape.

(55) Chabal, Y. J. *Surf. Sci. Rep.* **1988**, *8*, 211−357.

Practically, integrated absorbances have been extracted from the data by fitting the experimental vibrational signals to simple line shapes. To obtain a reliable determination, it appears mandatory to fit the spectral baseline and the vibrational line(s) in the region of interest simultaneously. The procedure is straightforward for the νCO mode, which is isolated and well characterized in the experimental spectra. In this case, we used a Lorentzian profile to fit the data (for the surface layer and for the calibration as well). It is worth mentioning that the calibration should be performed using a dilute acid solution because the νCO infrared absorption is so intense that it significantly affects the refractive index of concentrated (or neat) acid solutions. Such sizable perturbations of the refractive index should be avoided because they violate at least two hypotheses of the above derivation: the negligible spectral dependence of the optical constants (other than the absorption coefficient) around the vibrational mode (used for integrated absorbances) and the close values of the real dielectric constant of the adsorbed layer and the refractive index of the liquid. Taking $C = 3.1 \times 10^{19}$ cm^{-3} (corresponding to the 1% vol solution of decanoic acid in dodecane that we have used) and $d = 0.47$ μm at 1715 cm^{-1}, we end up with the following figures for the surface concentration of the carbonyl acid groups in the grafted layers (expressed in cm^{-2})

$$N_{\parallel} = A_s(7.9 \times 10^{15}) \text{ and } N_{\perp} = (2.19A_p - 1.98A_s)(6.7 \times 10^{15}) \quad \text{(A9)}$$

where $A_{s,p}$ stands for the integrated absorbance per reflection of the νCO mode (expressed in cm^{-1}) measured in s or p polarization, computed using the natural logarithm.

The situation is somewhat more complicated for the calibration of the νCH modes. This is primarily due to the fact that the νCH band is the superimposition of four fundamental vibrational modes: the symmetric and antisymmetric stretching modes of the CH_2 and CH_3 groups (except for pure acid layers where only CH_2 groups are present). The situation is further complicated by the presence of several combination bands enhanced by Fermi resonance. To keep the number of adjustable parameters to a minimum and end up with the most reliable determination of the infrared intensity of the fundamental modes, we adjust the whole νCH band to the superimposition of five Voigt profiles, with four of them accounting for the fundamental modes and the fifth accounting for the most salient combination band near 2900 cm^{-1}. The convergence of the fitting procedure is also oriented toward solutions while keeping a reasonable line width for all of the contributions (typically around 20 cm^{-1}) to minimize unphysical intensity transfers between the various contributions. In principle, the presence of several modes provides us with some redundant information. However, the reliability of the results is not identical for the various modes. First, CH_2 modes will be preferred because of the small abundance of methyl groups in decyl or mixed decyl/carboxydecyl layers. Moreover, the antisymmetric mode near 2920 cm^{-1} has been found to be more dependent on the fit details than its symmetric counterpart near 2850 cm^{-1}, though the calibrations performed with the two modes generally yield comparable values. The dispersion in the fit results is somewhat larger than 10% for the intensity of the asymmetric mode, whereas it remains below 5% for that of the symmetric mode. We therefore regard the intensity of the $\nu_s CH_2$ mode as the most reliable experimental quantity for measuring the surface concentration of methylene groups in the grafted layers. Taking $C = 2.7 \times 10^{22}$ cm^{-1} (corresponding to the concentration of CH_2 groups in dodecane) and $d = 0.29$ μm at 2850 cm^{-1}, we end up with the following figures for the surface concentration of methylene groups in the grafted layer (expressed in cm^{-2})

$$N_{\parallel} = A_s(2.0 \times 10^{17}) \text{ and } N_{\perp} = (2.19A_p - 1.98A_s)(1.7 \times 10^{17}) \quad \text{(A10)}$$

where $A_{s,p}$ stands for the integrated absorbance per reflection of the $\nu_s CH_2$ mode (expressed in cm^{-1}) measured in s or p polarization, computed using the natural logarithm.

For example, from Figure 1b, the integrated intensity of the $\nu_s CH_2$ mode was found to be 12.6×10^{-3} in s polarization and 12.7×10^{-3} in p polarization. From these numbers and using eq A10, we deduced $N_{\parallel} = 2.33 \times 10^{15}$ cm^{-2} and $N_{\perp} = 0.44 \times 10^{15}$ cm^{-2}, leading to $N = 2.77 \times 10^{15}$ cm^{-2} and a surface concentration of grafted decyl chains of 3.08×10^{14} cm^{-2}.

LA052145V